Convective Heat Transfer in a High Aspect Ratio Minichannel Heated on One Side

Convective Heat Transfer in a High Aspect Ratio Minichannel Heated on One Side

Eric C. Forrest[1]
Primary Standards Laboratory,
Sandia National Laboratories,
Albuquerque, NM 87185
e-mail: ecforre@sandia.gov

Lin-Wen Hu
Mem. ASME
Nuclear Reactor Laboratory,
Massachusetts Institute of Technology,
Cambridge, MA 02139
e-mail: lwhu@mit.edu

Jacopo Buongiorno
Mem. ASME
Department of Nuclear Science and Engineering,
Massachusetts Institute of Technology,
Cambridge, MA 02139
e-mail: jacopo@mit.edu

Thomas J. McKrell
Department of Nuclear Science and Engineering,
Massachusetts Institute of Technology,
Cambridge, MA 02139
e-mail: tmckrell@mit.edu

Experimental results are presented for single-phase heat transfer in a narrow rectangular minichannel heated on one side. The aspect ratio and gap thickness of the test channel were 29:1 and 1.96 mm, respectively. Friction pressure drop and Nusselt numbers are reported for the transition and fully turbulent flow regimes, with Prandtl numbers ranging from 2.2 to 5.4. Turbulent friction pressure drop for the high aspect ratio channel is well-correlated by the Blasius solution when a modified Reynolds number, based upon a laminar equivalent diameter, is utilized. The critical Reynolds number for the channel falls between 3500 and 4000, with Nusselt numbers in the transition regime being reasonably predicted by Gnielinski's correlation. The dependence of the heat transfer coefficient on the Prandtl number is larger than that predicted by circular tube correlations, and is likely a result of the asymmetric heating. The problem of asymmetric heating condition is approached theoretically using a boundary layer analysis with a two-region wall layer model, similar to that originally proposed by Prandtl. The analysis clarifies the influence of asymmetric heating on the Nusselt number and correctly predicts the experimentally observed trend with Prandtl number. A semi-analytic correlation is derived from the analysis that accounts for the effect of aspect ratio and asymmetric heating, and is shown to predict the experimental results of this study with a mean absolute error (MAE) of less than 5% for $4000 < Re < 70{,}000$. [DOI: 10.1115/1.4031646]

Keywords: narrow rectangular channel, parallel plates, minichannel, single-phase heat transfer, secondary flow, turbulent flow, critical Reynolds number, asymmetric heating, test reactor

Introduction

The use of closely spaced, plate-type fuel elements developed for materials test reactors (MTRs) results in coolant channel geometries which are rectangular and very narrow. Convective heat transfer studies in narrow rectangular channels are limited compared to those in circular geometries. The primary reason is that few high heat transfer applications use rectangular cooling geometries. Circular tubes are easier to fabricate than rectangular ducts, are more suited for service at elevated pressure, and typically offer lower overall thermal and flow resistances for the system. In addition, experimental investigation of heat transfer in rectangular channels is more difficult in regards to fabrication, testing, and measurement.

The hydraulic diameter is a useful parameter when dealing with flow in noncircular conduits for the purpose of characterizing hydrodynamic and heat transfer phenomena

$$D_{\text{hyd}} = \frac{4A_{\text{flow}}}{P_w} \tag{1}$$

In the case of a circular tube, the hydraulic diameter reduces to the tube diameter. The rectangular channels in MTRs are commonly characterized by very high aspect ratios. A schematic of a prototypic geometry is shown in Fig. 1. w is the dimension of the long wall and t_{gap} is the dimension of the short wall. The inverse aspect ratio is

$$\alpha^* = \frac{t_{\text{gap}}}{w} \tag{2}$$

In the case that $w \gg t_{\text{gap}}$, $\alpha^* \longrightarrow 0$ and the hydraulic diameter simplifies to

$$D_{\text{hyd,r.c.}} = \frac{4A_{\text{flow}}}{P_w} = \frac{4wt_{\text{gap}}}{2w + 2t_{\text{gap}}} \xrightarrow{w \gg t_{\text{gap}}} 2t_{\text{gap}} \tag{3}$$

This result is equivalent to that for parallel plates, where $\alpha^* = 0$. Therefore, experimental investigations of heat transfer in parallel plate geometries can be relevant to very narrow rectangular coolant channel geometries. In the case where the coolant channel geometry has some curvature, such as in many MTRs, the parallel plate approximation may still be suitable if the radius of curvature of the fuel plates is much greater than the coolant channel gap.

Kandlikar introduced a fixed metric classifying channels based on size [1,2], where minichannels are defined as having a minimum channel dimension less than 3 mm. Based on this classification, the coolant channels in many MTRs are minichannels. While

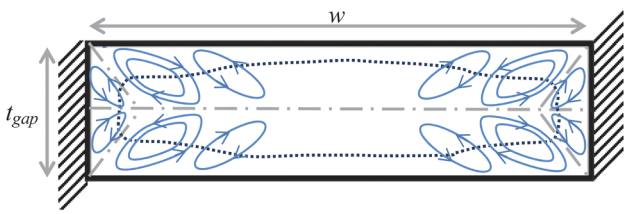

Fig. 1 Schematic of rectangular channel geometry, showing typical secondary flow profile. The dotted line represents an isovelocity line of the primary flow profile (flowing into the page). The arrows represent secondary flows, with the flow direction perpendicular to the primary flow. Adapted from Ref. [3].

[1]Corresponding author.

Contributed by the Heat Transfer Division of ASME for publication in the JOURNAL OF HEAT TRANSFER. Manuscript received October 20, 2014; final manuscript received September 16, 2015; published online October 21, 2015. Assoc. Editor: Ali Khounsary.

there has been substantial interest in microchannels for heat transfer applications in recent years, rectangular minichannels have largely been overlooked. The majority of prior studies involving high aspect ratio minichannels involve low mass flux and narrow ranges of the Prandtl number, with air as the working fluid. Growing interest in compact heat exchangers for power generation applications could lead to increased study for these types of channels over a broader range of flow conditions and Prandtl numbers.

Rectangular channels also exhibit secondary flows, as illustrated qualitatively in Fig. 1. While the magnitude of these secondary flows may only be around 1/10th of the primary flow velocity, their presence results in increased friction pressure drop when compared to circular tubes of equal hydraulic diameter. The turbulent friction factor is known to increase monotonically with increasing aspect ratio when the Reynolds number and hydraulic diameter are kept constant [4]. Additionally, the potential for asymmetric heating and nonuniform velocity profiles may further complicate heat transfer predictions for narrow rectangular channels. Therefore, the suitability of using circular tube correlations to predict heat transfer in high aspect ratio, narrow rectangular channels is debatable.

Historical Review

Historically, circular tube correlations have been applied to high aspect ratio, narrow rectangular channels in the prediction of turbulent single-phase heat transfer. Circular tube correlations continue to be used for design and safety analyses of MTR coolant channels. The McAdams correlation [5], commonly referred to as the Dittus–Boelter equation (though it differs from the correlation developed by Dittus and Boelter [6]), has been used in prior safety analyses for the MIT Research Reactor (MITR). A modified Colburn equation, proposed by Stoever [7], was recommended by the Phillips Reactor Safeguards Committee for the MTR [8]. However, as early as 1959, studies were conducted to assess the suitability of applying circular tube heat transfer results to high aspect ratio rectangular channels. Levy et al. [9] specifically investigated the issue for MTRs, with Levy noting that there was essentially no data available for such channels. Levy measured single-phase heat transfer and the critical heat flux (CHF) in a rectangular channel, reporting turbulent forced convection heat transfer rates 30–45% below that predicted by Sieder–Tate, and 15–30% lower than that predicted by most other circular tube correlations. Levy also found the CHF to be significantly lower than that for circular tubes. The poor heat transfer characteristics reported by Levy were the primary driver for a study by Gambill and Bundy [10] in support of the High Flux Isotope Reactor (HFIR) design. In this study, Gambill identified potential issues with the setup used by Levy et al., such as heat flux peaking in the channel corners. The single-phase heat transfer coefficients measured in Gambill's experiments were 10–20% greater than that predicted by the Sieder–Tate correlation.

Experimental studies investigating single-phase heat transfer in similar narrow channels were conducted at MIT in the late 1960 s and early 1970 s to support the MITR core redesign [11,12]. One of the MIT studies provides results for smooth channels, finding the single-phase heat transfer coefficient to be 12% greater than that predicted by the modified Colburn correlation, which was previously used in the safety analysis for the High Flux Beam Reactor (HFBR) [13]. A more recent study by Sudo et al. [14] investigated both laminar and turbulent flow for upflow and downflow in a narrow rectangular channel meant to simulate a coolant channel of the JRR-3. Unlike prior studies, the short walls of Sudo's channel were not heated, more closely replicating the actual heating geometry in MTRs. Above a Reynolds number of 10,000, Sudo's results display a spread of approximately ±20%, making it difficult to draw firm conclusions with respect to circular tube predictions. Sudo simply recommends use of the Dittus–Boelter equation (the McAdams correlation) for predicting turbulent single-phase heat transfer in such channels.

The results of studies investigating turbulent single-phase heat transfer in narrow rectangular channels, with specific application to MTRs, are summarized in Table 1. Note that with the exception of the data presented by Levy and Sudo, the measured turbulent single-phase heat transfer coefficient is greater than that predicted by circular tube correlations. However, the Reynolds and Prandtl number ranges investigated were limited in the studies, making it difficult to develop a robust correlation for the narrow geometries.

While many other studies have investigated heat transfer in rectangular channels, few approach aspect ratios as small as that considered here or have heating conditions and Prandtl numbers similar to those of this study. Much of the work done in rectangular channels has been done for air, with $Pr < 1$. A study by Sparrow and Cur [15] investigated mass transfer in a rectangular

Table 1 Summary of studies investigating various heat transfer phenomena in narrow rectangular channels for MTR applications

Institution/reactor	Year	Geometry	Re	P, T	Parameter studied	Result	Reference
GE and KAPL	1959	Rectangular channel; $t_{gap} = 0.1$ in.; $L \times w$: 2.5 in. × 18 in./36 in.; vertical flow	6000–200,000	4.5–13.8 bar; 20–134 °C	$h_{1\phi}$, CHF	$h_{1\phi}$ 15–45% less than c.t. correlations; CHF values 1/3 of those predicted by c.t. correlations	[9]
ORNL/HFIR	1961	Rectangular channel; $t_{gap} = 0.043$ in. −0.0057 in.; $L \times w$: 18 in. × 1.06 in.; upflow	9000–270,000	1.0–39.5 bar	f, $h_{1\phi}$, CHF	$h_{1\phi}$ 10–20% greater than Sieder–Tate equation; CHF accurately predicted by Zenkevich–Subbotin correlation	[10]
MIT/MITR	1969	Rectangular channel; $t_{gap} = 0.090$ in.; $L \times w$: 2.5 in. × 24 in.; upflow	6500–20,000	∼1 bar, < 60 °C	$h_{1\phi}$	$h_{1\phi}$ 12% greater than modified Colburn correlation	[11]
MIT/MITR	1975	Rectangular channel; $D_{hyd} = 2.16$ mm; upflow	∼2200–14,000	∼1 bar, <60 °C	$h_{1\phi}$	Results for finned channel only	[12]
JAERI/JRR-3	1984	Rectangular channel; $t_{gap} = 2.25$ mm; $L \times w$: 50 mm × 750 mm; upflow/downflow	∼100–50,000	<42°	$h_{1\phi}$	Turbulent flow: large spread in $h_{1\phi}$ (± 20%), but recommends Dittus–Boelter; laminar flow: new correlation	[14]

channel with $\alpha^* = 0.0556$ and $10{,}000 < \mathrm{Re} < 45{,}000$. The gap of the channel was approximately 2 cm, significantly larger than that found in MTRs. Although the working fluid was a naphthalene–air system, studies were conducted at a fixed Schmidt number of $\mathrm{Sc} = 2.5$. For heating on both sides (uniform wall temperature conditions), they found that the Sherwood number could be related to the Reynolds number by

$$\mathrm{Sh} = 0.05\,\mathrm{Re}^{0.76} \tag{4}$$

The Chilton–Colburn analogy relates the Sherwood number to the Nusselt number [16], giving us

$$j_h = \frac{\mathrm{Nu}}{\mathrm{RePr}^{1/3}} = j_{\mathcal{M}} = \frac{\mathrm{Sh}}{\mathrm{ReSc}^{1/3}} \tag{5}$$

In the original paper by Chilton and Colburn, Eq. (5) is stated as being valid for $0.7 \leq \mathrm{Pr} \leq 1000$. Using the Chilton–Colburn analogy, we can infer from the results of Sparrow and Cur a relation for the Nusselt number at the fixed Prandtl number of $\mathrm{Pr} = 2.5$

$$\mathrm{Nu} = 0.05\,\mathrm{Re}^{0.76} \tag{6}$$

Since the study of Sparrow and Cur is only applicable for a single Prandtl number, no Prandtl dependence can be inferred for their channel or heating conditions. However, if we assume the dependence of the Nusselt number on the Prandtl number to be similar to the Colburn correlation (i.e., $\mathrm{Nu} \propto \mathrm{Pr}^{1/3}$), then a general correlation for a high aspect ratio rectangular channel heated on both sides with isothermal wall conditions can be formulated as

$$\mathrm{Nu} = 0.036\,\mathrm{Re}^{0.76}\mathrm{Pr}^{1/3} \tag{7}$$

Note that Eq. (7) is based off mass transfer measurements for a naphthalene–air system at a single Schmidt number. Also note that the wall conditions were isothermal (unlike in this study), and for a channel with a substantially larger gap than in MTRs, so Eq. (7) should be used with caution.

While data for rectangular channels at relevant Reynolds and Prandtl numbers are sparse, turbulent heat transfer studies with parallel plates are more abundant. As noted earlier, parallel plate studies (where $\alpha^* = 0$) should be applicable to heat transfer in MTR-type coolant channels away from the channel edges. Bhatti and Shah [3] summarize heat transfer results for parallel plates, noting that in the range $10{,}000 < \mathrm{Re} < 30{,}000$ and $0.5 < \mathrm{Pr} < 100$, the Nusselt number is up to 1.23 times that predicted by circular tube correlations.

Furthermore, a number of analytical and semi-analytical studies have been conducted for the parallel plate geometry. In 1961, Barrow [17] published analytical results for the case of turbulent flow between parallel plates with each wall having unequal but uniform heat fluxes. For the case of one-sided heating, the Nusselt number calculated by Barrow is

$$\mathrm{Nu} = \frac{0.1986\,\mathrm{Re}^{7/8}\mathrm{Pr}}{10.06\,\mathrm{Re}^{1/8} + 9.74(\mathrm{Pr} - 2)} \tag{8}$$

Barrow claims his theoretical analysis is valid for Pr greater than about 0.7, as he assumes that eddy conductivity is constant in his analysis. Barrow also assumes that the thickness of the viscous sublayer is small compared with the channel gap. Sparrow and Lin [18] also performed an analytical study for a parallel plate configuration with Pr from 0.7 to 100 and Re from 10,000 to 500,000. Sparrow and Lin presented their results graphically, noting that from their solution, the Nusselt number dependence on the Prandtl number is more complex than a simple power law, which is that typically encountered in empirical correlations. Note that for Prandtl numbers relevant to this study, the analytic solution of Sparrow and Lin predicts Nusselt numbers higher than those predicted by the McAdams correlation. Sakakibara and Endo [19] proposed a numerical solution to the parallel plate problem with a uniform wall temperature boundary condition and provided the necessary constants and eigenvalues for different Pr and Re in a tabular format.

Experimental Apparatus

A thermal-hydraulic test loop was constructed to accommodate a high aspect ratio, rectangular channel simulating coolant channels found in MTRs. A schematic of the test loop is provided in Fig. 2. The loop was constructed using 300 series stainless steel with hard fluoroelastomer seals where needed to reduce contaminants in the deionized water stream. A bellows-type accumulator acts as a system pressurizer and thermal expansion compensator. A 1-hp centrifugal pump allows for mass fluxes up to 7000 $\mathrm{kg/m^2}$ s through the test section. A four-pass shell-and-tube heat exchanger transfers heat to the building chilled water system. System flow rate is measured using a vortex meter. Test section and heat exchanger inlet and outlet temperatures are measured using four-wire platinum resistance temperature detectors (RTDs). A solenoid valve on the chilled water system, along with a preheater, allows for fully automated control of system temperatures via a proportional-integral-derivative (PID) controller.

The test section consists of a vertical, narrow rectangular channel uniformly heated on one side. The heater and test section were modeled using COMSOL and finite-element analysis tools in MATLAB to ensure a constant wall heat flux and predict maximum temperatures and thermal gradients. Fabrication tolerances accounted for the anticipated thermal expansion of components at operating temperatures. Transition sections, cut using wire electrical discharge machining (EDM), form a smooth inlet and exit to the channel to reduce vortex shedding and reduce the required hydrodynamic development length. A photograph and computer aided design (CAD) model of the test section are provided in Fig. 3.

The test section is instrumented with absolute pressure transducers after the test section inlet and before the outlet. A differential pressure transducer is also installed to permit accurate measurement of friction pressure drop during testing. The heated side of the channel consists of a 316 stainless steel plate seated in a high-performance fluoropolymer insulator. The plate is heated resistively using a 72 kW DC power supply capable of supplying 4500 A at 16 V. Current is measured using a Hall effect current transducer, while voltage is measured from taps on the heater electrodes. Current is delivered to the heater plate using a copper busbar and four 2000 MCM welding cables. Eighteen type E thermocouples measure the temperature on the backside of the heater plate. The heater surface temperature is calculated by accounting for measured thermal contact resistances of each installed thermocouple, and determining the temperature drop in the plate for uniform internal heat generation. The entire facility is controlled using National Instruments LABVIEW, with data collected through an Agilent 34980 A Multifunction measurement unit. The general parameters of the flow facility and test section are summarized in Table 2.

The surface finish of the channel was carefully controlled, with the heater plate prepared to match the average roughness values measured on actual MTR cladding. In general, the surface roughness of the plate is not expected to have an influence on single-phase heat transfer as long as it can be considered hydraulically smooth, such that the characteristic roughness of the surface is small compared to the thickness of the viscous sublayer. Typically, the root-mean-square (RMS) roughness, R_{rms}, is used as the roughness length scale for this comparison. For the heater plate of this study, the RMS surface roughness was measured using confocal microscopy and found to be $R_{\mathrm{rms}} \approx 0.7\,\mu\mathrm{m}$. For the range of conditions tested, the estimated sublayer thickness ranged from about 10 μm to 70 μm, so the flow can be treated as hydraulically smooth. Similarly, the Moody diagram [20] may be referenced, showing that an RMS roughness of 0.7 μm would not be expected to have an appreciable effect on the friction factor, and therefore should have little effect on the heat transfer coefficient.

All single-phase experiments were conducted using deionized water, with a measured electrical resistivity greater than 15 MΩ cm. The water and surface were degassed prior to taking measurements. Tests were conducted for each bulk fluid temperature condition by increasing the mass flux in a stepwise fashion. The heat flux was set such that the wall-to-bulk temperature difference was 10 °C or less, in order to keep the wall viscosity influence on the heat transfer coefficient at less than 3%, as estimated using the relation introduced by Sieder and Tate. At each mass flux, sufficient time was taken for the temperature of the system to achieve steady-state conditions. Measurements were recorded for 10 min at each steady-state condition. The local conditions at each thermocouple along the center of the channel were calculated individually. For thermocouples near the inlet and outlet of the test section, higher values of the heat transfer coefficient were usually observed, with behavior also being less consistent compared to the middle of the channel. This is likely due to flow development and disturbance near the inlet and outlet.

The heat rate to the fluid, and associated surface heat flux, were determined from the enthalpy rise in the test section. Heat loss to ambient was determined by comparing the total electric power to the thermal power and was typically less than 10%. Where possible, the accuracy of test and measurement equipment was verified by the experimentalist by calibrating against known standards. Uncertainties were accounted for and propagated using former practices recommended by the ASME and ANSI [21,22]. All dimensional tolerances were also accounted for in the uncertainty analysis. Uncertainties are expressed at the 95% confidence level. Fundamental uncertainties for various measurements are listed in Table 3. Typical repeatability of the measured heat transfer coefficient was 5% or better. The ultimate uncertainty in the reported Nusselt number was usually around ±10%, except at high mass fluxes where a small temperature rise and increased variability led to higher fractional uncertainties.

Results

Friction Pressure Drop. The friction pressure gradient along a channel may be expressed as

$$-\left(\frac{dP}{dz}\right)_{\text{friction}} = \frac{1}{2} f \frac{\rho u_b^2}{D_{\text{hyd}}} \tag{9}$$

where f is the Darcy friction factor. In laminar flow, an exact solution for the velocity profile, and therefore the friction factor, is available for circular tubes, parallel plates, and rectangular channels. For parallel plates, the Darcy friction factor for fully developed, laminar flow is

$$f = \frac{96}{\text{Re}} \tag{10}$$

In the case of rectangular channels, the aspect ratio is a relevant parameter in laminar flow, with the analytical solution for the fully developed friction factor being [23]

$$f = \frac{96}{(1+1/\alpha^*)^2 \left[1 - \frac{192}{\pi^5 \alpha^*} \sum_{n=1,3,\ldots}^{\infty} \frac{1}{n^3} \tanh\left(\frac{n\pi\alpha^*}{2}\right)\right] \text{Re}} \tag{11}$$

In our case, the inverse aspect ratio, α^*, is 0.035 and the friction factor for laminar flow is therefore

$$f = \frac{91.67}{\text{Re}} \tag{12}$$

For turbulent flow, circular tube correlations are typically used with the hydraulic diameter in place of the tube diameter. Blasius provided the following relation for the fully developed, turbulent friction factor in a smooth tube [24]:

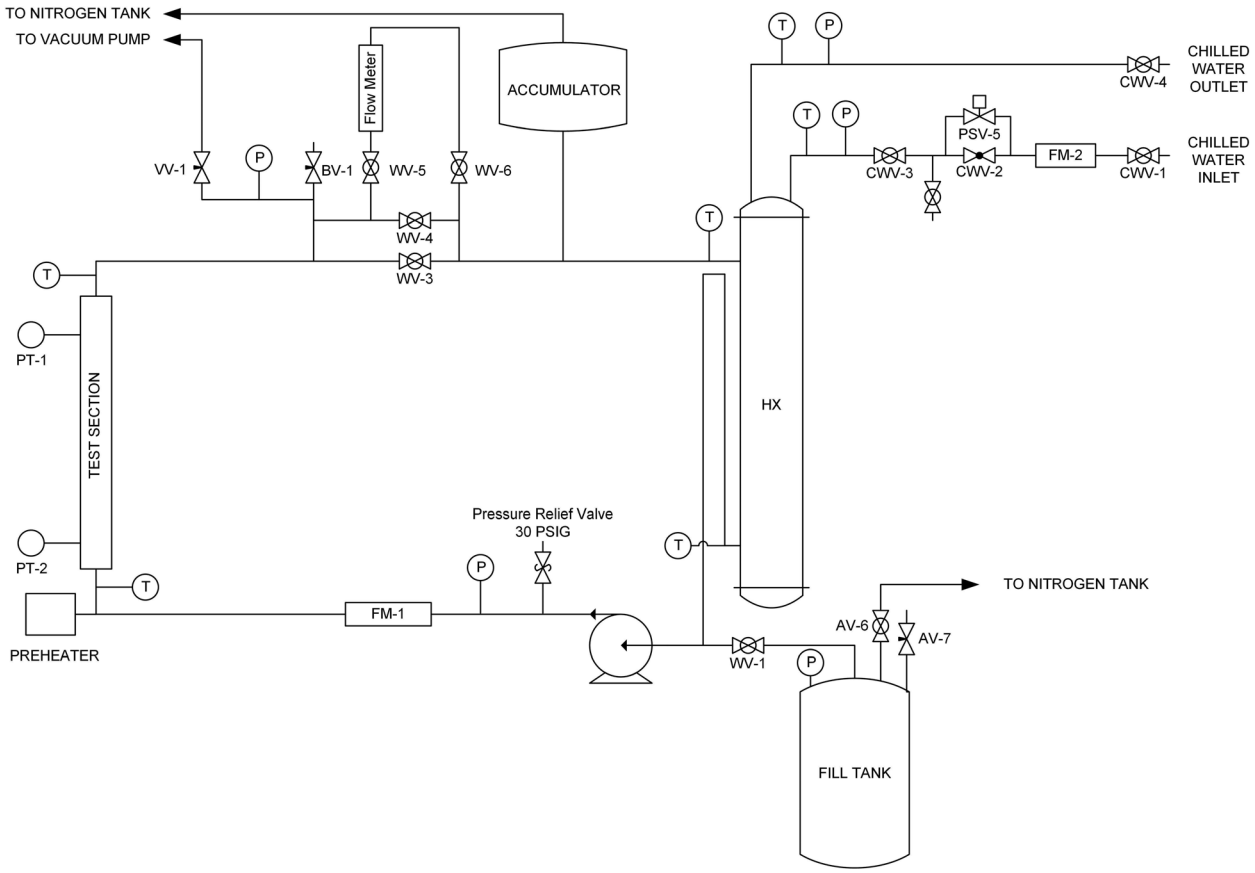

Fig. 2 Schematic of the thermal-hydraulic test facility

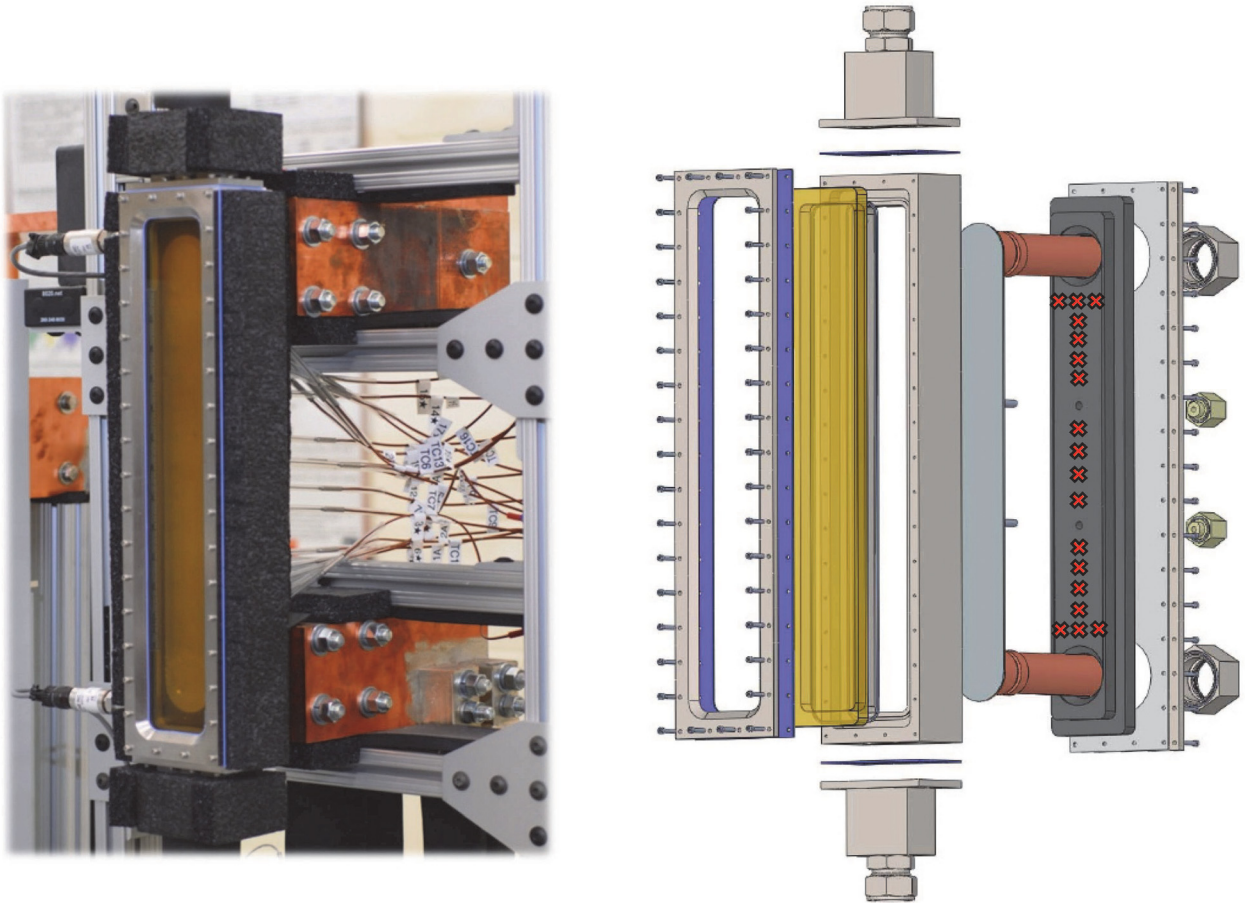

Fig. 3 The narrow rectangular coolant channel test section. The channel is heated on one side, with a polysulfone viewing window on the front face. Thermocouple locations are indicated by X's in the CAD model on the right.

$$f = 0.3164\,\mathrm{Re}^{-0.25} \tag{13}$$

with Eq. (13) being applicable for turbulent flow with $\mathrm{Re} > 3000$.

In studying turbulent friction factors, Jones postulated that the standard hydraulic diameter may not be the correct dimension to obtain geometric similarity between round and rectangular ducts [4]. Jones points to the example of the effect of increasing aspect ratio on the measured friction factor, which is not captured by the standard hydraulic diameter. Using an analytic comparison between circular and rectangular geometries in laminar flow, and empirical data for turbulent flow, Jones introduces a modified Reynolds number and laminar equivalent diameter

$$\mathrm{Re}^* = \phi^* \mathrm{Re}_{D_{\mathrm{hyd}}} \tag{14}$$

$$D_L = \phi^* D_{\mathrm{hyd}} \tag{15}$$

where D_{hyd} is the standard hydraulic diameter, calculated by Eq. (1), and ϕ^* is a geometry function, which is exactly equal to

$$\phi^* = \frac{2}{3}\left(1 + \frac{t_{\mathrm{gap}}}{w}\right)^2 \times \left[1 - \frac{192 t_{\mathrm{gap}}}{\pi^5 w}\sum_{n=0}^{\infty}\frac{1}{(2n+1)^5}\tanh\left\{\frac{(2n+1)\pi w}{2t_{\mathrm{gap}}}\right\}\right] \tag{16}$$

Equation (16) may be approximated by

$$\phi^* \approx \frac{2}{3} + \frac{11}{24} \times \frac{t_{\mathrm{gap}}}{w}\left(2 - \frac{t_{\mathrm{gap}}}{w}\right) \tag{17}$$

In this study, the pressure drop across the channel was measured using the differential pressure transducer. When accounting for the gravity head, the difference between the absolute transducers was in excellent agreement with the differential transducer. The measured friction factor, based upon measurements with the differential transducer, is plotted in Fig. 4. The correlations plotted for laminar and turbulent flow utilize the laminar equivalent diameter concept introduced by Jones and are calculated using Re*. Note that the use of 64/Re* for laminar flow yields a result equivalent to Eq. (12). As shown in Fig. 4, the friction factor is

Table 2 Test section and flow loop parameters

Parameter	Value
Channel gap, t_{gap}	1.96 mm
Channel width, w	55.9 mm
Hydraulic diameter, D_{hyd}	3.79 mm
Inverse aspect ratio, α^*	0.035
Heated width, w_H	51.0 mm
Channel length, L	482.6 mm
Heated length, L_H	304.8 mm
Inlet pressure, P_{in}	up to 3.08 bar
Inlet temperature, T_{in}	up to 99 °C
Mass flux, G	up to 7000 kg/m^2 s
Surface heat flux, q''	up to 3.8 MW/m^2
Laplace length, L_p	2.55–2.77 mm
Dimensionless length, L/D_{hyd}	127
Prandtl number, Pr	1.77–9.44
Reynolds number, Re	2200–93,000

Table 3 Summary of fundamental measurement uncertainties for the thermal-hydraulic facility and test section. Uncertainties represent 95% confidence bounds.

Parameter	Total uncertainty	Notes
Primary current, I_P	$\pm 1\%$ full scale (FS) $= \pm 60$ A	For current transducer; offset corrected for separately
Voltage drop, V_E	$\pm[0.005\%$ of reading $+ 4 \times 10^{-6}]$ V	Data acquisition system voltage channel
Current signal, I	5.5×10^{-5} A	Data acquisition system 4–20 mA channel
Type E TC temperature, T	$\pm 0.297\,^{\circ}$C	Total uncertainty of least accurate thermocouple on backside of heater plate
RTD temperature, T_{in}, T_{out}	$\pm 0.156\,^{\circ}$C	Total uncertainty of least accurate RTD used for inlet and outlet fluid temperature measurements
Differential RTD temperature, ΔT	$\pm 0.052\,^{\circ}$C	Maximum deviation + random uncertainty of inlet and outlet RTD
Primary flow rate, Q_p	$\varepsilon_m = \pm 5.68$ gpm/A $\varepsilon_b = \pm 0.068$ gpm	Uncertainty in slope and intercept of fitted calibration curve
Absolute pressure, P	$\pm 0.25\%$ FS $= \pm 0.125$ psia (± 0.0086 bar)	Includes linearity, repeatability, and hysteresis
Differential pressure, P	$\pm 0.25\%$ FS $= \pm 0.025$ psia (± 0.0017 bar)	Includes linearity, repeatability, and hysteresis

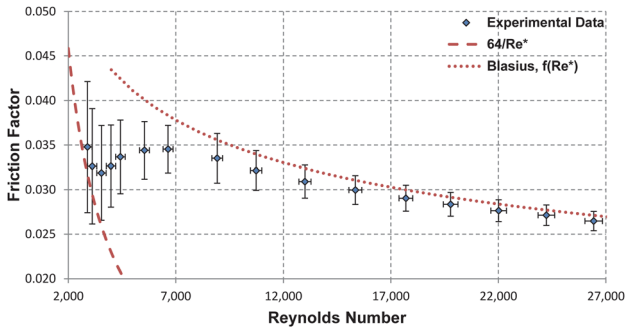

Fig. 4 Experimental friction factor as a function of Reynolds number. The corresponding predictions for laminar flow (analytic result) and turbulent flow (Blasius equation), calculated using Re*, are plotted for comparison. Error bars represent total uncertainty at the 95% confidence level.

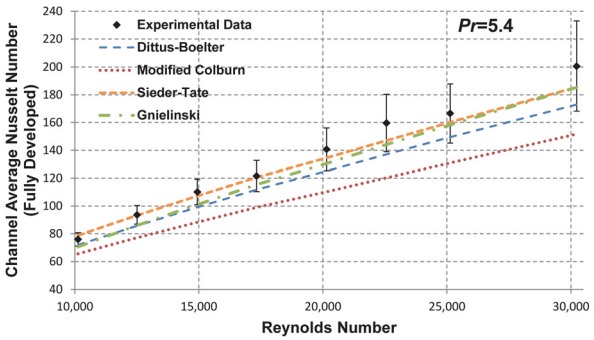

Fig. 6 Fully developed, average channel Nusselt numbers for Pr = 5.4 in a high aspect ratio, narrow rectangular channel heated on one side. Error bars represent total uncertainty at the 95% confidence level.

predicted adequately when the modified Reynolds number is used. Otherwise, the friction factor would be underpredicted by about 20% for the high aspect ratio channel.

Low Reynolds Number Heat Transfer (Re < 10,000). The critical Reynolds number, below which the flow remains laminar, depends on a number of factors in rectangular channels, including aspect ratio and entrance configuration. Note that flow may remain laminar to much higher Re under appropriate vibration-free conditions in very smooth channels. The configuration of the experimental test section in this study most closely corresponds to the smooth entrance, whereas that in most MTRs corresponds to the abrupt entrance.

For this study, accurate measurements with Re < 2200 were not practical due to range limitations of the vortex flow meter. However, measurements were obtained for flows as low as Re ≈ 3800 for the heat transfer coefficient and ≈2900 for the friction factor. From the friction factor data in Fig. 4, the critical Reynolds number in this study falls between 3500 and 4000, or

$$\mathrm{Re}_{crit} = 3500 \ \text{ to } \ 4000 \tag{18}$$

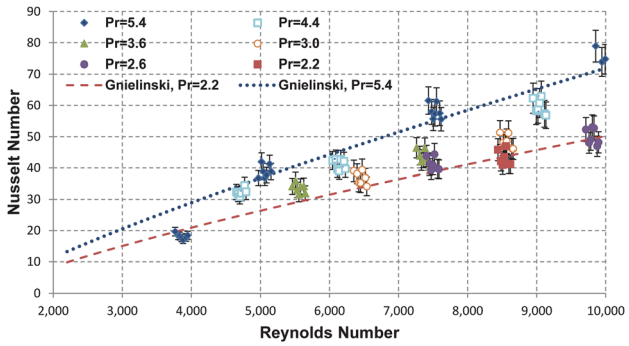

Fig. 5 Local fully developed Nusselt number results in the high aspect ratio, narrow rectangular channel heated on one side for Re < 10,000. Error bars represent measurement uncertainty at the 95% confidence level.

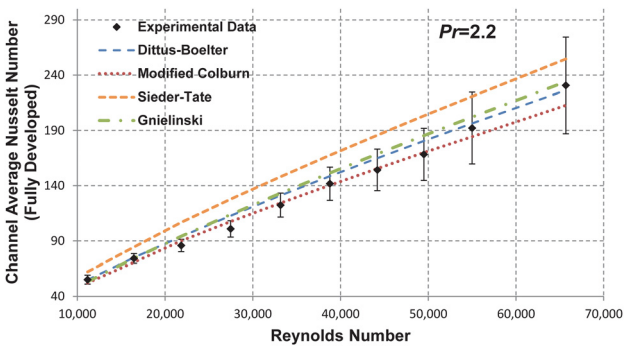

Fig. 7 Fully developed, average channel Nusselt numbers for Pr = 2.2. Error bars represent total uncertainty at the 95% confidence level.

which is consistent with the values reported by Bhatti and Shah [3] for high aspect ratio rectangular channels. The friction factor data also indicate that flow does not become fully turbulent until $Re \gtrsim 7000$.

The fully developed, single-phase heat transfer results for $Re < 10{,}000$ are summarized in Fig. 5 for the range of Prandtl numbers tested in this study. Even at the low end of the flow range, measured Nusselt numbers were quite repeatable. The Gnielinski correlation [25], which is considered applicable as low as $Re = 2100$, is also plotted for comparison at the highest and lowest Prandtl number. Note that the measured values in this range are, on average, 10.3% higher than that predicted by the Gnielinski correlation. Below $Re = 4000$, the Gnielinski correlation for $Pr = 5.4$ (top curve) overpredicts the Nusselt number by about 40% possibly indicating that the flow is still laminar in this region. Therefore, for conservatism, the laminar flow heat transfer prediction for rectangular channels should be used for $Re < 4000$, while the Gnielinski correlation may be used as a conservative estimate for $4000 < Re < 10{,}000$.

Fully Turbulent Heat Transfer (Re > 10,000). Results are presented in Figs. 6 and 7 for the highest and lowest Prandtl numbers tested with $Re > 10{,}000$. Each data point represents the average Nusselt number for flow at fully developed locations. Error bars represent 95% confidence limits for each measurement. Uncertainty in the Reynolds number was also accounted for, but is small and not shown for clarity. In total, six bulk temperature conditions were tested, consisting of $Pr_{avg} = 5.4$ ($T_b \approx 30\,^{\circ}C$), $Pr_{avg} = 4.4$ ($T_b \approx 40\,^{\circ}C$), $Pr_{avg} = 3.6$ ($T_b \approx 50\,^{\circ}C$), $Pr_{avg} = 3.0$ ($T_b \approx 60\,^{\circ}C$), $Pr_{avg} = 2.6$ ($T_b \approx 70\,^{\circ}C$), and $Pr_{avg} = 2.2$ ($T_b \approx 80\,^{\circ}C$). It is important to note that most data collected for $Re > 30{,}000$ was for lower Prandtl numbers, due to the viscosity reduction resulting in a higher Reynolds number for a given mass flux. The uncertainty in the measured Nusselt number was also higher at these conditions, due to the smaller temperature rise from the inlet to the outlet and between the bulk fluid and the surface.

Discussion

The one-sided, or asymmetric, heating condition, is frequently encountered in the end channels of an MTR fuel assembly. The end channel is often the limiting channel (hot channel) due to reduced flow and heat flux peaking caused by increased neutron moderation. Therefore, it is important to understand the influence of asymmetric heating on the Nusselt number and correlate the data appropriately. Since the heating condition at each wall of a rectangular channel imposes a boundary condition on the problem, it is expected that altering the boundary condition will affect the solution to the temperature profile. Consider, first, the case of the velocity profile. If the velocity profile is not coupled to the temperature profile, then the thermal boundary conditions will have no effect on the solution for velocity, resulting in a symmetric profile, with no difference whether there is no heating, heating on one side, or heating on both sides. In reality, the fluid properties change with temperature, which will have a small effect on the velocity profile.

Therefore, it can be said for turbulent flow that if the velocity boundary layer is thicker than the thermal boundary layer, then the heat transfer process is dominated by advection (i.e., $\delta_{hyd} > \delta_{th}$ or $Pr > 1$), and the influence of one-sided versus two-sided heating should be small. The same cannot be said for laminar or buoyancy-driven flows, where the effect of one-sided versus two-sided heating may be significant, as demonstrated by Sudo et al. [14].

Empirical results for turbulent flow in narrow channels support that the effect of one-sided versus two-sided heating on turbulent heat transfer is small for $Pr \gg 1$. Referring again to the mass transfer study of Sparrow and Cur [15], and also relying on the Chilton–Colburn analogy, their results for $Sc = 2.5$ indicate that the Nusselt number will be about 8% lower for one-sided versus two-sided heating when $Pr = 2.5$. For their turbulent heat transfer results, Sudo et al. [14] are not able to distinguish any difference between one-sided and two-sided heating in their prototypic MTR channel. In a semi-empirical study of flow in annular spaces, Kays and Leung [26] analytically extended their experimental results for heated annuli to the case of parallel plates, determining that the Nusselt number for one-sided heating is lower than that for heating on both sides, where the effect has a strong dependence on the Prandtl number. Using their tabulated solutions, it is possible to plot the ratio of Nusselt numbers for one-sided heating to two-sided heating, under otherwise similar conditions. These results are plotted in Fig. 8, showing the trend with Prandtl number for a range of Reynolds numbers. As expected, the ratio converges to unity with increasing Prandtl number, due to the increasing thickness of the velocity boundary layer relative to the thermal boundary layer. Though not shown in the graph, note that for very small Prandtl numbers, i.e., $Pr < 0.1$, the ratio approaches the asymptotic value of 0.53.

Empirical Fit of the Results. An empirical fit of the experimental data provides some insight into the general behavior with Reynolds and Prandtl number and the influence of one-sided heating. A power law is utilized for simplicity, but limited to the range of $10{,}000 \le Re \le 35{,}000$. The Reynolds number for the fit is limited to 35,000, since it was not possible to collect data for the

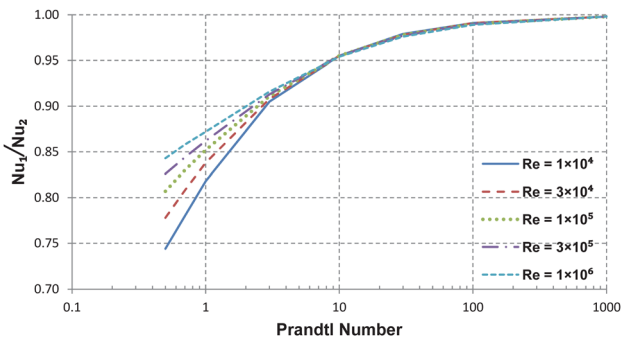

Fig. 8 Expected effect of one-sided versus two-sided heating for parallel plates. Expressed as the ratio of the Nusselt numbers for one-sided heating (Nu_1) and two-sided heating (Nu_2). Adapted from the tabular results of Ref. [26].

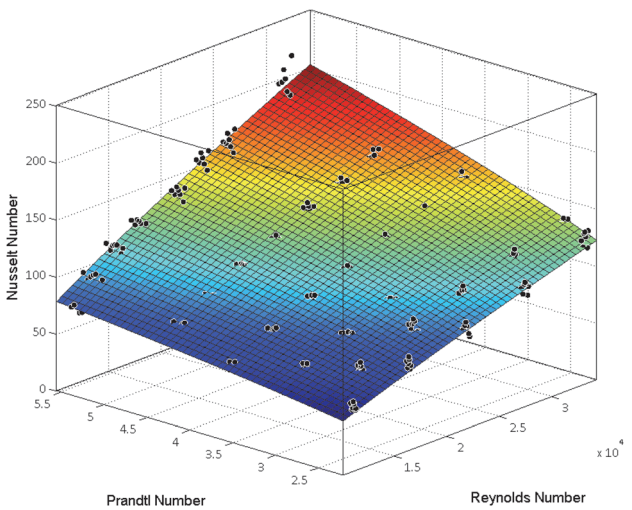

Fig. 9 Surface fitted to experimental data, represented by $Nu = 0.0242Re^{0.775}Pr^{0.548}$. The corresponding data range is $10{,}000 \le Re \le 35{,}000$ and $2.2 \le Pr \le 5.4$. The associated coefficient of determination is $R^2 = 0.9997$.

entire range of Prandtl numbers above $\mathrm{Re} = 35{,}000$. Using a robust least-squares regression method to reduce the effect of outlying data, a surface fit to the data yields the following correlation:

$$\mathrm{Nu} = 0.0242\ \mathrm{Re}^{0.775}\mathrm{Pr}^{0.548} \tag{19}$$

for $10{,}000 \le \mathrm{Re} \le 35{,}000$ and $2.2 \le \mathrm{Pr} \le 5.4$, which is applicable for fully developed flow away from the channel edges with $\alpha^* \approx 0.35$, heated on one side with uniform heat flux. Equation (19) should not be used outside of the specified Re and Pr range for which it was fit, since the data here and in other studies in the literature indicate a simple power law is not adequate for describing the behavior of Nu over a broader range in such channels. The surface of Eq. (19) with corresponding data is shown in Fig. 9.

Semi-Analytic Correlation. For flow at high Reynolds numbers, the thermal boundary layer may be characterized in a manner similar to the velocity boundary layer, with distinct regions near the wall. The thermal wall layer will display universal properties if it is within the velocity wall layer, which is the case when $\mathrm{Pr} \gtrapprox 0.5$ [27]. Using a two-layer approach, similar to that of Prandtl, the velocity boundary layer can be modeled as a laminar sublayer and a turbulent overlap layer that extends into the turbulent core, with the buffer layer essentially being neglected. Making several assumptions [28], the energy equation can be written as follows for the channel:

$$u\frac{\partial T}{\partial z} = \frac{\partial}{\partial y}\left[(\alpha + \varepsilon_H)\frac{\partial T}{\partial y}\right] \tag{20}$$

Ultimately, the temperature drop in each layer is desired. The temperature drop of each layer can be estimated using an approach similar to that used by Barrow [17], with some important differences. First, the dimensionless thickness of the laminar sublayer is updated from 9.74 to the now commonly accepted value of 5, such that

$$\delta_\nu^+ = \frac{y_1 u_\tau}{\nu} = 5 \tag{21}$$

Second, the velocity distribution is updated for the turbulent region. Finally, the Blasius solution for the friction factor is altered to rely upon the modified Reynolds number, such that

$$f = 0.3164[\phi^* \mathrm{Re}]^{-0.25} \tag{22}$$

Without going into detail, the following analytical solution for the Nusselt number may be derived, which accounts for the one-sided heating and the aspect ratio of the channel:

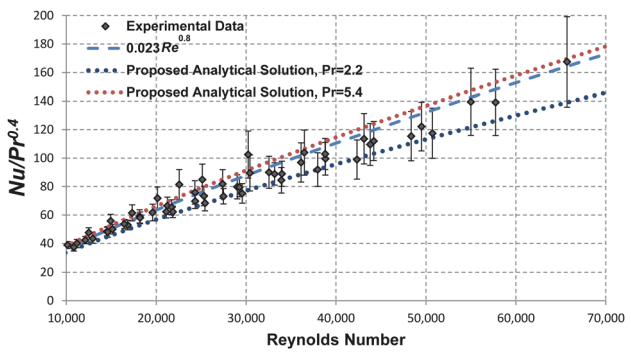

Fig. 10 Summary of experimental data for Re > 10,000 normalized by $\mathrm{Pr}^{0.4}$. The newly derived semi-analytical solution is plotted along with the McAdams correlation for the highest and lowest Prandtl numbers explored in this study.

$$\mathrm{Nu} = \frac{0.199\,\mathrm{Re}^{7/8}\,\mathrm{Pr}}{\delta_\nu^+[\mathrm{Pr} - 2]\phi^{*1/8} + 10.05\,\mathrm{Re}^{1/8}\phi^{*1/4}} \tag{23}$$

The complete derivation is available in Ref. [28]. The above equation is intended for turbulent flow in the center of the channel. In the form derived here, the dimensionless laminar sublayer thickness may be specified independently if a value other than $\delta_\nu^+ = 5$ is desired. Due to the assumptions made, the equation is only valid for $\mathrm{Pr} \gtrapprox 1$.

Despite the approximations made in the boundary layer analysis to derive this purely analytical solution, Eq. (23) yields an MAE of 4.1% in predicting experimental data within this study when $10{,}000 < \mathrm{Re} < 35{,}000$. In addition, the analytical solution derived above correctly predicts the behavior of the Nusselt number for $\mathrm{Re} > 30{,}000$. However, for the transition flow region, i.e., $4000 < \mathrm{Re} < 10{,}000$, the purely analytical correlation overpredicts the experimental data somewhat, with an MAE of 7.3%. It is possible to modify Eq. (23) to better account for the transition regime without significantly affecting the prediction when $\mathrm{Re} > 10{,}000$. In a similar manner to Gnielinski's modification of the Petukhov correlation [25], the Reynolds number term can be modified slightly. The resulting correlation, modified to improve accuracy in the transition region, may be written as

$$\mathrm{Nu} = \frac{0.199(\mathrm{Re} - 600)^{7/8}\mathrm{Pr}}{5[\mathrm{Pr} - 2]\phi^{*1/8} + 10.05(\mathrm{Re} - 600)^{1/8}\phi^{*1/4}} \tag{24}$$

This semi-analytic correlation predicts the experimental data for one-sided heating in the transition regime with an MAE of 4.2%. The MAE for the entire range of data, i.e., $4000 \le \mathrm{Re} \le 70{,}000$ and $2.2 \le \mathrm{Pr} \le 5.4$, is less than 4.6%. A summary of all experimental data where $\mathrm{Re} > 10{,}000$, normalized to $\mathrm{Pr}^{0.4}$, is plotted along with the Dittus–Boelter equation (McAdams correlation) in Fig. 10. The semi-analytical correlation proposed in Eq. (24) is also plotted for the upper and lower bounds of the Prandtl number explored in experiments.

A comparison of data to various correlations is provided in Table 4. Note the Reynolds and Prandtl number ranges over which the MAE was calculated. Based on the comparison, the semi-analytic correlation is recommended for transition and turbulent flows in high aspect ratio rectangular channels uniformly heated on one side. For two-sided heating, while no data were collected in this study, Fig. 8 can be consulted to provide an estimate of the expected effect on the Nusselt number.

Conclusions

An experimental study has been performed to measure the single-phase friction factor and Nusselt number for a high aspect ratio, rectangular minichannel heated on one side. The critical Reynolds number for the test section was found to be higher than that encountered in circular tubes, which was expected from the literature. The friction factor for the turbulent flow regime was also higher than that in circular tubes due to the presence of secondary flows, but is well-correlated when a modified Reynolds number based on a laminar equivalent diameter concept is employed. Single-phase heat transfer in the turbulent flow regime was not predicted adequately by circular tube correlations, requiring modification of the Reynolds number to capture aspect ratio effects on heat transfer. Heat transfer also exhibited a strong dependence on the Prandtl number and did not obey a simple power relation, likely due to the asymmetric heating condition. A semi-analytic correlation was developed for the case of one-sided heating which accounts for the aspect ratio of the channel. The new correlation predicts the experimental single-phase Nusselt number with an MAE of less than 5% in the range of $4000 \le \mathrm{Re} \le 70{,}000$ and $2.2 \le \mathrm{Pr} \le 5.4$.

Table 4 Summary of MAEs of various correlations in predicting the single-phase data for the channel heated on one side.

Correlation	Equation	Re range	MAE (%), $2.2 \leq Pr \leq 5.4$
McAdams (Dittus–Boelter)	Ref. [5]	10,000–70,000	6.4
Modified Colburn	Refs. [7] and [8]	10,000–70,000	7.3
Sieder and Tate	Refs. [5] and [29]	10,000–70,000	15.2
Gnielinski	Ref. [25]	10,000–70,000	8.4
Petukhov	Ref. [30]	10,000–70,000	11.4
Modified Sparrow and Cur	(7)	10,000–70,000	6.1
Barrow (one-sided)	(8)	10,000–70,000	20.4
Fitted empirical correlation	(19)	10,000–35,000	3.8
Semi-analytic correlation	(24)	4,000–70,000	4.6

Acknowledgment

Yakov Ostrovsky and Dr. David Carpenter of MIT NRL are gratefully acknowledged for their assistance with the test section fabrication and LABVIEW programming, respectively. The comments from Professor Neil Todreas of MIT and Dr. Hy Tran, Nishant Patel, Roger Burton, and Dr. Eric Detlefs of the Primary Standards Laboratory are greatly appreciated. This research was performed under appointment to the U.S. Department of Energy Nuclear Nonproliferation Safeguards Graduate Fellowship Program sponsored by the National Nuclear Security Administration's Office of Nonproliferation and International Security. The experimental program was sponsored by the National Nuclear Security Administration's Global Threat Reduction Initiative through Argonne National Laboratory, Contract No. 25-30101-0004 A. Sandia National Laboratories is a multiprogram laboratory managed and operated by Sandia Corporation, a wholly owned subsidiary of Lockheed Martin Corporation, for the U.S. Department of Energy's National Nuclear Security Administration under Contract No. DE-AC04-94AL85000. This publication has been approved for unlimited public release, SAND2014-18834 J.

Nomenclature

A_{flow} = flow area (m^2)
c_p = specific heat capacity (J/kg K)
$\mathcal{D}$ = diffusion coefficient (m^2/s)
D_{hyd} = hydraulic diameter (m)
D_L = laminar equivalent diameter (m)
f = Darcy friction factor
g = acceleration due to gravity (m/s^2)
G = mass flux (kg/m^2 s)
h = heat transfer coefficient (W/m^2 K)
I = current (A)
j_h = Colburn factor, $\equiv Nu/RePr^{1/3}$
$j_{\mathcal{M}}$ = Colburn factor, $\equiv Sh/ReSc^{1/3}$
k = thermal conductivity (W/m K)
$\mathcal{K}$ = mass transfer coefficient (m/s)
L = length (m)
L_p = Laplace length (m)
n = number
Nu = Nusselt number, $\equiv hD_{hyd}/k$
P = pressure (Pa, bar, or psi)
P_w = wetted perimeter (m)
Pr = Prandtl number, $\equiv \mu c_p/k$
q'' = heat flux (W/m^2)
Q = volumetric flow rate (m^3/s or gpm)
R_{rms} = root-mean-square roughness (μm)
R^2 = coefficient of determination
Re = Reynolds number, $\equiv \rho u D_{hyd}/\mu$
Re* = modified Reynolds number, $\equiv \phi^* Re$
Sc = Schmidt number, $\equiv \mu\rho/\mathcal{D}$
Sh = Sherwood number, $\equiv \mathcal{K}D_{hyd}/\mathcal{D}$
T = temperature (°C or K)
t_{gap} = gap thickness (m)
u = flow velocity magnitude in primary (z) direction (m/s)
u_τ = friction velocity (m/s)
V_E = voltage drop (V)
w = width (m)
y = thickness (depth) coordinate (m)
z = axial (length) coordinate (m)

Greek Symbols

α = thermal diffusivity (m^2/s)
α^* = inverse aspect ratio
δ_{hyd} = velocity boundary layer thickness (m or μm)
δ_{th} = thermal boundary layer thickness (m or μm)
δ_v = viscous (laminar) sublayer thickness (m or μm)
δ_v^+ = dimensionless viscous sublayer thickness
Δ = difference
ε = uncertainty (at 95% confidence level)
ε_H = eddy diffusivity of heat (m^2/s)
μ = viscosity (Pa·s)
ν = kinematic viscosity (m^2/s)
ρ = density (kg/m^3)
ϕ^* = geometry function

Subscripts

avg = average
b = bulk
b = intercept
c.t. = circular tube
H = heated
hyd = hydrodynamic, hydraulic
in = inlet
m = slope
out = outlet
p = primary
r.c. = rectangular channel
th = thermal
1 = outer edge of laminar sublayer
1ϕ = single phase

References

[1] Kandlikar, S. G., and Grande, W. J., 2003, "Evolution of Microchannel Flow Passages—Thermohydraulic Performance and Fabrication Technology," Heat Transfer Eng., **24**(1), pp. 3–17.
[2] Kandlikar, S. G., 2006, *Heat Transfer and Fluid Flow in Minichannels and Microchannels*, Elsevier, Amsterdam, p. 3.
[3] Bhatti, S., and Shah, R. K., 1987, "Turbulent and Transition Flow Convective Heat Transfer in Ducts," *Handbook of Single-Phase Convective Heat Transfer*, S. Kakaç, R. K. Shah, and W. Aung, eds., Wiley, New York, pp. 4.62–4.77.
[4] Jones, O. C., Jr., 1976, "An Improvement in the Calculation of Turbulent Friction in Rectangular Ducts," ASME J. Fluids Eng., **98**(2), pp. 173–180.
[5] McAdams, W. H., 1942, *Heat Transmission*, 2nd ed., McGraw-Hill, New York, pp. 167–168.
[6] Dittus, F. W., and Boelter, L. M. K., 1930, "Heat Transfer in Automobile Radiators of the Tubular Type," Univ. Calif. Publ. Eng., **2**(13), pp. 443–461. (Reprinted in International Communications in Heat and Mass Transfer, 12, pp. 3–22.)
[7] Stoever, H. J., 1944, "Heat Transfer: Conduction, Radiation and Convection," Chem. Metall. Eng., **51**(5), pp. 98–107.
[8] Nertney, R. J., 1957, "Calculated Surface Temperatures for Nuclear Systems and Their Uncertainties," Atomic Energy Division, Phillips Petroleum Co., AEC Research and Development Report No. IDO-16343.
[9] Levy, S., Fuller, R. A., and Niemi, R. O., 1959, "Heat Transfer to Water in Thin Rectangular Channels," ASME J. Heat Transfer, **81**(2), pp. 129–143.
[10] Gambill, W. R., and Bundy, R. D., 1961, "HFIR Heat-Transfer Studies of Turbulent Water Flow in Thin Rectangular Channels," Oak Ridge National Laboratory, Oak Ridge, TN, Technical Report No. ORNL-3079.
[11] Spurgeon, D., 1969, "Preliminary Design Studies for a High Flux MIT Reactor," M.S./Nuc. Eng. thesis, Massachusetts Institute of Technology, Cambridge, MA.
[12] Szymczak, W. J., 1975, "Experimental Investigation of Heat Transfer Characteristics of MITR-II Fuel Plates, In-Channel Thermocouple Response and

Calibration," M.S./Nuc. Eng. thesis, Massachusetts Institute of Technology, Cambridge, MA.
[13] Hendrie, J. M., 1964, "Final Safety Analysis Report on the Brookhaven High Flux Beam Research Reactor," Brookhaven National Laboratory, Upton, NY, Technical Report No. BNL-7661(Vol.I).
[14] Sudo, Y., Miyata, K., Ikawa, H., Ohkawara, M., and Kaminaga, M., 1985, "Experimental Study of Differences in Single-Phase Heat Transfer Characteristics Between Upflow and Downflow for Narrow Rectangular Channel," J. Nucl. Sci. Technol., **22**(3), pp. 202–212.
[15] Sparrow, E., and Cur, N., 1982, "Turbulent Heat Transfer in a Symmetrically or Asymmetrically Heated Flat Rectangular Duct With Flow Separation at Inlet," ASME J. Heat Transfer, **104**(1), pp. 82–89.
[16] Chilton, T. H., and Colburn, A. P., 1934, "Mass Transfer (Absorption) Coefficients: Prediction From Data on Heat Transfer and Fluid Friction," Ind. Eng. Chem., **26**(11), pp. 1183–1187.
[17] Barrow, H., 1961, "Convection Heat Transfer Coefficients for Turbulent Flow Between Parallel Plates With Unequal Heat Fluxes," Int. J. Heat Mass Transfer, **1**(4), pp. 306–311.
[18] Sparrow, E. M., and Lin, S. H., 1963, "Turbulent Heat Transfer in a Parallel-Plate Channel," Int. J. Heat Mass Transfer, **6**(3), pp. 248–249.
[19] Sakakibara, M., and Endo, K., 1976, "Analysis of Heat Transfer for Turbulent Flow Between Parallel Plates," Int. Chem. Eng., **16**(4), pp. 728–733.
[20] Moody, L., 1944, "Friction Factors for Pipe Flow," Trans. ASME, **66**(8), pp. 671–684.
[21] ANSI/ASME PTC 19.1-1985, 1986, *Measurement Uncertainty*, Part I, American Society of Mechanical Engineers, New York.
[22] Kim, J. H., Simon, T. W., and Viskanta, R., 1993, "Editorial—Journal of Heat Transfer Policy on Reporting Uncertainties in Experimental Measurements and Results," ASME J. Heat Transfer, **115**(1), pp. 5–6.
[23] Shah, R. K., and London, A. L., 1971, "Laminar Flow Forced Convection Heat Transfer and Flow Friction in Straight and Curved Ducts—A Summary of Analytical Solutions," Office of Naval Research, Arlington, VA, Technical Report No. 75.
[24] Blasius, H., 1912, "Das Aehnlichkeitsgesetz bei Reibungsvorgängen," Z. Ver. Dtsch. Ing., **56**(16), pp. 639–643.
[25] Gnielinski, V., 1976, "New Equations for Heat and Mass Transfer in Turbulent Pipe and Channel Flow," Int. Chem. Eng., **16**(2), pp. 359–368.
[26] Kays, W., and Leung, E., 1963, "Heat Transfer in Annular Passages—Hydrodynamically Developed Turbulent Flow With Arbitrarily Prescribed Heat Flux," Int. J. Heat Mass Transfer, **6**(7), pp. 537–557.
[27] Schlichting, H., and Gersten, K., 2000, *Boundary-Layer Theory*, 8th ed., (translated by K. Mayes), Springer-Verlag, Berlin, pp. 551–605.
[28] Forrest, E. C., 2014, "Study of Turbulent Single-Phase Heat Transfer and Onset of Nucleate Boiling in High Aspect Ratio Mini-Channels to Support the MITR LEU Conversion," Ph.D. thesis, Massachusetts Institute of Technology, Cambridge, MA.
[29] Sieder, E. N., and Tate, G. E., 1936, "Heat Transfer and Pressure Drop of Liquids in Tubes," Ind. Eng. Chem., **28**(12), pp. 1429–1435.
[30] Petukhov, B. S., 1970, "Heat Transfer in Turbulent Pipe Flow With Variable Physical Properties," Adv. Heat Transfer, **6**, pp. 503–564.